



**University of
Zurich**^{UZH}

**Zurich Open Repository and
Archive**

University of Zurich
University Library
Strickhofstrasse 39
CH-8057 Zurich
www.zora.uzh.ch

Year: 2010

Scattered light fluorescence microscopy: imaging through turbid layers

Vellekoop, I M ; Aegerter, C M

Abstract: A major limitation of any type of microscope is the penetration depth in turbid tissue. Here, we demonstrate a fundamentally novel kind of fluorescence microscope that images through optically thick turbid layers. The microscope uses scattered light, rather than light propagating along a straight path, for imaging with subwavelength resolution. Our method uses constructive interference to focus scattered laser light through the turbid layer. Microscopic fluorescent structures behind the layer were imaged by raster scanning the focus.

DOI: <https://doi.org/10.1364/OL.35.001245>

Posted at the Zurich Open Repository and Archive, University of Zurich

ZORA URL: <https://doi.org/10.5167/uzh-36763>

Journal Article

Accepted Version

Originally published at:

Vellekoop, I M; Aegerter, C M (2010). Scattered light fluorescence microscopy: imaging through turbid layers. *Optics Letters*, 35(8):1245-1247.

DOI: <https://doi.org/10.1364/OL.35.001245>

Scattered light fluorescence microscopy: imaging through turbid media

Ivo M. Vellekoop^{1,*} and Christof M. Aegerter^{1,2}

¹*Physik Institut, Universität Zürich, Winterthurerstrasse 190, CH-8057 Zürich, Switzerland*

²*Fachbereich Physik, Universität Konstanz, Universitätsstrasse 10, 78457 Konstanz, Germany*

**Corresponding author: ivo.vellekoop@physik.uzh.ch*

A major limitation of any type of microscope is the penetration depth in turbid tissue. Here, we demonstrate a fundamentally novel kind of fluorescence microscope that images through optically thick turbid layers. The microscope uses scattered light, rather than light propagating along a straight path, for imaging with sub-wavelength resolution. Our method uses constructive interference to focus scattered laser light through the turbid layer. Microscopic fluorescent structures behind the layer were imaged by raster-scanning the focus. © 2010 Optical Society of America

OCIS codes: 290.4210, 110.0180, 110.7050, 030.6140.

The fluorescence microscope has become an indispensable tool in any biological or medical laboratory. The development of fluorescent genetic constructs [1] has revolutionized cell- and developmental biology, and in-vivo fluorescent markers are playing an increasing role in biomedical imaging [2]. Currently, one of the main limitations of even the most advanced microscopes is the penetration depth in turbid materials [3]. This limitation is fundamentally due to the fact that inside a turbid medium small particles and imperfections scatter the light before it reaches the desired image plane.

There are tremendous ongoing efforts in improving the imaging depth and resolution of fluorescence microscopes. Historically, two approaches can be identified. The first is to form an image using the fraction of the light that is not scattered. This so-called ballistic light propagates along a straight line and converges to a sharp focus. The difficulty lies in rejecting or reducing the undesired contribution of the scattered light. Notable examples of this category are confocal fluorescence microscopy and multi-photon microscopy [4].

The second approach is to record the scattered light and then use advanced inversion schemes to reconstruct the fluorescent structure. This way it is possible to image up to

tens of centimeters deep in, for instance, human tissue [5], or resolve mesoscopic details in developing fruit flies [6]. However, the very nature of these methods limits the resolution: details with sizes comparable to the wavelength of the light cannot be resolved.

In parallel to these research efforts, methods were developed to focus laser light through turbid materials. Recent examples include turbidity suppression through optical phase conjugation [7], time reversal of electromagnetic radiation [8], and spatial wavefront shaping [9,10]. These methods have in common that the incident wave is shaped spatially and/or temporally to match the exact scattering behavior of the material. The shaped wave scatters in such a way that it interferes constructively at the desired point, effectively creating a focus. Since it is interference of the scattered light forming the focus, these methods can be summarized as ‘interferometric focusing’, as opposed to the geometric focusing of a lens.

Here we demonstrate experimentally the first scanning fluorescence microscope based on interferometric focusing. Our technique, called scattered light fluorescence microscopy (SLFM) uses scattered light to form an image with sub-wavelength resolution. The principle of SLFM is depicted in Fig. 1. Given a fluorescent structure that is hidden behind a turbid layer, conventional imaging fails because all incident light is scattered by the layer (Fig. 1a). First, one of the above mentioned methods is used to interferometrically focus the light through the scattering layer (Fig. 1b). Once the focus is formed, the incident wave uniquely matches the microscopic structure of the layer. Thus the focus is lost when the layer is moved. However, we found that, as a result of the optical memory effect, [11–13] the focus survives when the incident beam is *rotated*. For the purpose of microscopy, this effect allows raster-scanning the focus by tilting the incident wave (Fig. 1c). When the focus scans over a fluorescent particle, the total amount of fluorescence emitted by the sample peaks. This way, we are able to image fluorescent structures right through the scattering layer. Moreover, because the excitation light is focused sharply, the structures are resolved at high resolution, even when the fluorescent light is diffuse.

In our experiment we used spatial wavefront shaping [9] to form the initial focus. The incident light wave is shaped with a spatial light modulator (SLM). For a specific configuration of the SLM, the light will focus through the scattering layer. To find this configuration, a simple feedback algorithm [9] programs the SLM to maximize the intensity in the desired focal point. Although wavefront shaping has conceptual and instrumental similarities with adaptive optics, wavefront shaping is essentially a single-wavelength optical method, designed for a situation that is rarely considered in adaptive optics [14]: that of strong multiple scattering and diffraction on sub-wavelength-sized particles.

In this first demonstration of SLF microscopy we used feedback from a microscope that was placed behind the sample and, therefore, had direct optical access to the focal plane. Eventually, the initial focus would be created without optical access, for instance by using

a recently demonstrated technique that uses fluorescence from an embedded particle as feedback [15].

The schematic of our prototype SLF microscope is depicted in Fig. 1d. A polarized laser beam (Spectra-Physics Cyan 40 mW, 488 nm) is expanded and passes through a galvometer scanner (General Scanning LDS-07-OH). The exit aperture of the scanner is imaged onto a computer controlled SLM (Holoeye HEO 1080 P reflective phase only modulator). A lens and a $10\times$ microscope objective (Zeiss A-Plan $10\times/0.25$) image the surface of the SLM onto the sample surface. Note that even without scattering layer no focus would be formed. The feedback signal for forming the initial focus comes from a CCD camera that monitors the intensity in a 235 nm-radius spot at the back surface of the sample. This signal is used only for creating the initial focus.

After the focus is formed, we scan it over an area of $24 \times 24 \mu\text{m}^2$ by tilting the incident beam with the scanner. A photomultiplier tube behind the sample measures the total amount of fluorescence coming from the scanned area. A Semrock GFP-3035B filter set was used to reject the pump light. The scan signal is converted to an image and filtered with a 2-dimensional low pass filter to reduce photomultiplier noise. Forming the focus and scanning each take about 15 minutes, which currently limits the method to solid samples.

We tested the SLF microscope on a sample consisting of a $5.1 \pm 1.1 \mu\text{m}$ -thick layer of zinc oxide pigment (average particle diameter 200 nm) on a 1-mm-thick glass slide. This opaque white layer has a transport mean free path of $0.75 \pm 0.15 \mu\text{m}$, as derived from total transmission measurements. No transmitted ballistic light could be observed. A structure consisting of green fluorescent particles (Thermo Scientific 200 nm diameter polystyrene Firefli-dyed nanobeads) was placed at 1 mm behind the scattering layer, that is, on the other side of the glass slide.

Figure 2a shows a reference image of the fluorescent structure, taken from the back of the sample with a widefield fluorescence microscope. The structure is about $14 \mu\text{m}$ wide and has details that are smaller than the wavelength (488 nm) of the excitation light. Since the scattering layer is far thicker than the mean free path, conventional imaging through the layer is not possible. When one tries to image the structure with a fluorescence microscope, only a diffuse spot can be seen, as is shown in Figure 2b. Imaging with a confocal microscope did not work because the pinhole in the microscope rejected all scattered light, leaving no signal at all.

Fig. 2c shows the image that was obtained using SLF microscopy. Our method produces a high-resolution, high-contrast image of the fluorescent structure, where both widefield fluorescence microscopy and confocal microscopy fail. The scan image matches the reference image qualitatively very well. The distribution of the intensity differs slightly between the two images, possibly because of a slight focus drift between the measurements. Figure 2c

thus shows that it is possible to image right through a turbid layer without suffering from the effects of scattering.

To determine the resolution of the SLF microscope, we use a sample where the fluorescent beads have not clustered together. The scattering layer on this sample was even thicker than in the sample discussed above ($L = 12.1 \mu\text{m}$). The resulting image is shown in Fig. 3a: the three beads are resolved sharply. Fig. 3b shows the intensity profile of one of the beads. The profile has a full width at half maximum of $0.6 \mu\text{m}$. Already without compensating for the 200 nm diameter of the fluorescent bead itself, this result gives the microscope a resolving power of 300 nm , i. e. smaller than the wavelength of the light (488 nm). This resolution is comparable to that of a widefield fluorescence microscope in a perfectly clear medium. Imaging at such a high resolution through a scattering medium with a thickness of 16 mean free paths is unprecedented. Clearly, the turbid layer does not reduce the resolution of the image. In fact, since the light is focused by the turbid layer itself, the sharpness of the focus is not limited by the microscope objective in any way [16] and the resolution of a SLF microscope can, in principle, exceed that of the objective it uses.

The field of view of the microscope is determined by the angular range of the memory effect. The angle at which the focus intensity has decreased by a factor of e is in the order of $\alpha \approx \lambda/(2\pi L)$ [12,13]. Here, λ is the wavelength of the excitation light and L is the thickness of the scattering layer. It follows that SLF microscopy has the maximum field of view in an ‘egg’ geometry with the object of interest far behind a thin scattering layer. For the $5.1 \mu\text{m}$ -thick sample we expect a scan range of $\pm 15 \mu\text{m}$.

We have reported a fundamentally new approach to imaging in turbid media. SLF microscopy is able to image fluorescent structures hidden behind optically thick layers of scattering material. Our microscope resolves details with sub-wavelength accuracy through turbid layers of up to 16 transport mean free paths thick. At the moment, the main limitation of SLF microscopy is the need for access to the focal plane to construct the initial focus. This limitation can be overcome by using a recently demonstrated technique where the fluorescence of an embedded probe particle is used as feedback for the wavefront shaping procedure [15]. Combining this known technology with our SLF microscope will make it possible to perform truly non-invasive fluorescence imaging through extremely turbid layers. Areas of application include imaging of development processes, which typically take place inside egg, larval or pupal shells, as well as non-biological imaging of features inside structured materials or microscopic devices.

We thank Allard P. Mosk for valuable discussions. This work was supported by SystemsX.ch within the framework of the WingX RTD. IMV is supported by a ‘Forschungskredit’ of the University of Zurich.

References

1. D. J. Stephens and V. J. Allan, “Light Microscopy Techniques for Live Cell Imaging,” *Science* **300**, 82–83 (2007).
2. V. Ntziachristos, “Fluorescence Molecular Imaging,” *Annu. Rev. Biomed. Eng.* **8**, 1–33 (2006).
3. F. Helmchen and W. Denk, “Deep tissue two-photon microscopy,” *Nat. Methods* **2**, 932–940 (2005).
4. A. Diaspro, ed., *Confocal and Two-Photon Microscopy: Foundations, Applications and Advances* (Wiley-Liss, New York, 2002).
5. A. Corlu, R. Choe, T. Durduran, M. A. Rosen, M. Schweiger, S. R. Arridge, M. D. Schnall, and A. G. Yodh, “Three-dimensional in vivo fluorescence diffuse optical tomography of breast cancer in humans,” *Opt. Expr.* **15**, 6696–6716 (2007).
6. C. Vinegoni, C. Pitsouli, D. Razansky, N. Perrimon, and V. Ntziachristos, “In vivo imaging of *Drosophila melanogaster* pupae with mesoscopic fluorescence tomography,” *Nat. Methods* **5**, 45–47 (2008).
7. Z. Yaqoob, D. Psaltis, M. S. Feld, and C. Yang, “Optical phase conjugation for turbidity suppression in biological samples,” *Nat. Photonics* **2**, 110–115 (2008).
8. G. Lerosey, J. de Rosny, A. Tourin, and M. Fink, “Focusing Beyond the Diffraction Limit with Far-Field Time Reversal,” *Science* **315**, 1120–1122 (2007).
9. I. M. Vellekoop and A. P. Mosk, “Focusing coherent light through opaque strongly scattering media,” *Opt. Lett.* **32**(16), 2309–2311 (2007).
10. S. M. Popoff, G. Lerosey, R. Carminati, M. Fink, A. Boccaro, and S. Gigan, “Measuring the Transmission Matrix in Optics: An Approach to the Study and Control of Light Propagation in Disordered Media,” *Phys. Rev. Lett.* **104**, 100601 (2010).
11. D. L. Fried, “Anisoplanatism in adaptive optics,” *J. Opt. Soc. Am.* **72**, 52 (1982).
12. S. Feng, C. Kane, P. A. Lee, and A. D. Stone, “Correlations and Fluctuations of Coherent Wave Transmission through Disordered Media,” *Phys. Rev. Lett.* **61**, 834–837 (1988).
13. I. Freund, M. Rosenbluh, and S. Feng, “Memory Effects in Propagation of Optical Waves through Disordered Media,” *Phys. Rev. Lett.* **61**, 2328–2331 (1988).
14. R. K. Tyson, *Principles of Adaptive Optics* (Academic Press, New York, 1998).
15. I. M. Vellekoop, E. G. van Putten, A. Lagendijk, and A. P. Mosk, “Demixing light paths inside disordered metamaterials,” *Opt. Expr.* **16**(1), 67–80 (2008).
16. I. M. Vellekoop, A. Lagendijk, and A. P. Mosk, “Exploiting disorder for perfect focusing,” *Nat. Photonics*, accepted (2010).

List of Figures

- 1 (Color online) Principle of scattered light fluorescence microscopy. (a) A turbid layer blocks a fluorescent structure from sight, all incident light is scattered. (b) Using interferometric focusing (e. g. phase conjugation or wavefront shaping) scattered light is made to focus through the layer. (c) Imaging: the focus follows rotations of the incident beam. The hidden structure is imaged by scanning the focus. (d) Experimental setup. A laser beam is raster-scanned and its wavefront is shaped with a spatial light modulator (SLM). Dotted lines are conjugate planes. For ease of view, the SLM is drawn as a transmissive device and folding mirrors are omitted. 7
- 2 (Color online) Dense cluster of 200-nm-diameter fluorescent beads. (a) Seen directly (from the back of the sample) with a widefield fluorescence microscope, no scattering layer between the structure and the microscope. (b) Seen through the 5.1 μm -thick scattering layer with a widefield fluorescence microscope. The structure lies 1 mm below the layer. Only a diffuse spot, much larger than the fluorescent structure, is visible. Square box: area scanned with the SLF microscope. (c) Seen through the scattering layer with the SLF microscope. The structure is clearly visible at a high resolution. The image was mirrored for ease of comparison with (a). 8
- 3 (Color online) Resolution of the SLF microscope. (a) SLFM image of three 200-nm-diameter fluorescent beads, seen through a 12.1 μm layer of zinc oxide pigment. Scale bar is 1 μm . (b) Intensity profile of the lower right spot, indicating the resolution. 9

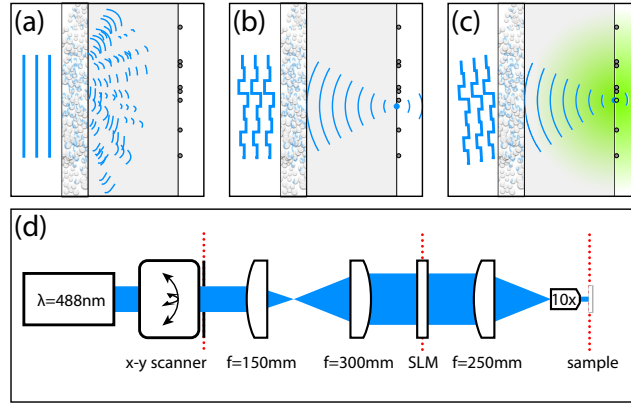


Fig. 1. (Color online) Principle of scattered light fluorescence microscopy. (a) A turbid layer blocks a fluorescent structure from sight, all incident light is scattered. (b) Using interferometric focusing (e. g. phase conjugation or wavefront shaping) scattered light is made to focus through the layer. (c) Imaging: the focus follows rotations of the incident beam. The hidden structure is imaged by scanning the focus. (d) Experimental setup. A laser beam is raster-scanned and its wavefront is shaped with a spatial light modulator (SLM). Dotted lines are conjugate planes. For ease of view, the SLM is drawn as a transmissive device and folding mirrors are omitted.

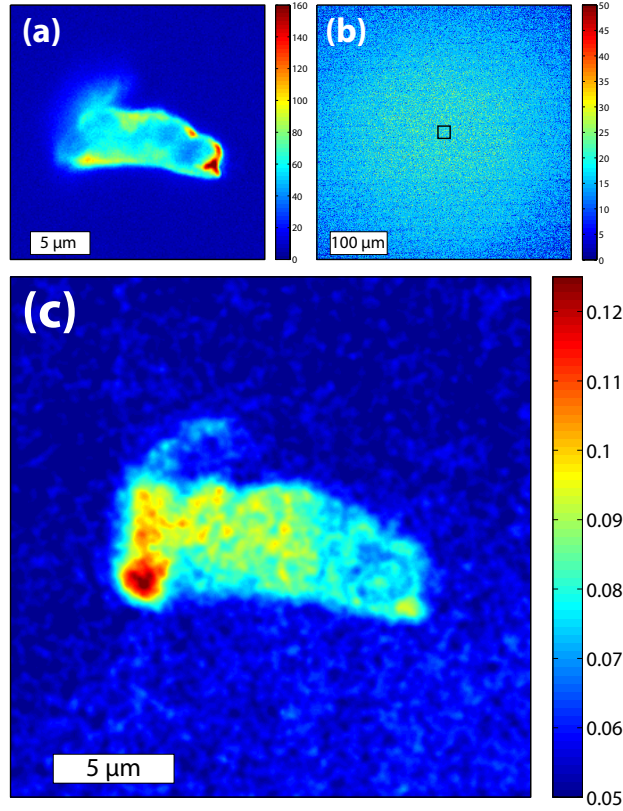


Fig. 2. (Color online) Dense cluster of 200-nm-diameter fluorescent beads. (a) Seen directly (from the back of the sample) with a widefield fluorescence microscope, no scattering layer between the structure and the microscope. (b) Seen through the 5.1 μm -thick scattering layer with a widefield fluorescence microscope. The structure lies 1 mm below the layer. Only a diffuse spot, much larger than the fluorescent structure, is visible. Square box: area scanned with the SLF microscope. (c) Seen through the scattering layer with the SLF microscope. The structure is clearly visible at a high resolution. The image was mirrored for ease of comparison with (a).

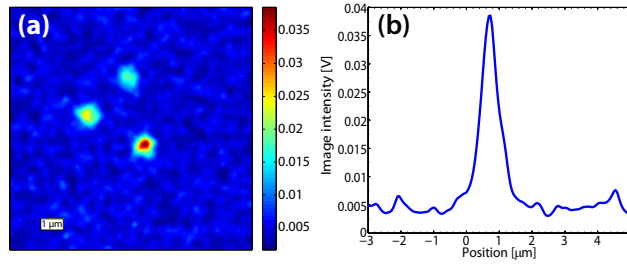


Fig. 3. (Color online) Resolution of the SLF microscope. (a) SLFM image of three 200-nm-diameter fluorescent beads, seen through a $12.1\ \mu\text{m}$ layer of zinc oxide pigment. Scale bar is $1\ \mu\text{m}$. (b) Intensity profile of the lower right spot, indicating the resolution.